International Journal of Core Engineering & Management
Volume-7, Issue-04, 2022 ISSN No: 2348-9510

PASSIVE MORPHING HEAT-SINK ARCHITECTURE USING BIO-INSPIRED VARIABLE-GEOMETRY FINS FOR TRANSIENT THERMAL LOADS A SYSTEMATIC REVIEW

Rupesh Rameshrao Dhore
Catia Designer
Altair Product Design Inc.
Canton, MI, USA
rupeshdhorey@gmail.com

Abstract

It is difficult to dissipate transient thermal loads from bursty electronic operation by conventional heat sinks sized for steady operation. This systematic review collects and combines 26 sources published since 2002 on the thermal buffering, the conductivity enhancement, the shape memory alloy thermal actuation, the constructal and bio-inspired geometry, and the electronics thermal problems associated with the use of the phase change material (PCM). The sources were organized into five thematic categories and integrated into a conceptual passive morphing heat-sink architecture with SMAs creating fins in response to base temperature which would increase the conductance to a phase change material without sensor or electrical power. In order to compare the performance of fixed fins without storage, fixed fins with storage, and morphing fins with storage, a lumped energy-balance model with ranges of properties consistent with the literature reviewed was used for the 25 watt, 300 second burst. Peak base temperature was estimated as 116.8°C, 57.0°C and 48.4°C for the no-storage, fixed-fins and storage, and morphing fins, respectively, at the end of the burst, and the fraction of the storage material that melted at the end of the burst increased from 41 percent to 49 percent. The three main challenges are hysteresis, fatigue, supercooling and experimental verification of the effective conductivity of the foam enhanced composites, which was estimated to be between 7.7 and 20.2 W/km for an assumed 5% solid fraction, and of neat paraffin, which was estimated to be around 0.2 W/km. Experimental directions for the future work are identified.

Index Terms—Passive morphing, heat sink, bio-inspired fins, phase change material, shape memory alloy, transient thermal load, constructal design, thermal management, electronics cooling.

I. INTRODUCTION

Thermal load is unique in electronic equipment because they are transient, or bursty. If this occurs, the heat released by the conventional heat sink is only at a steady rate, and the peak excursion is determined by the thermal capacitance, rather than the steady convective

International Journal of Core Engineering & Management
Volume-7, Issue-04, 2022 ISSN No: 2348-9510

conductance. These excursions were explored experimentally with the use of compact heat sinks with a phase change material (PCM) between their fins and it was shown that the temperature increase during heating could be delayed by using the finned PCM configuration [1].

The more it is concentrated, the more the problem is intensified. Heat fluxes at the chip level, which were of the order of 100 W/cm2, were discussed and it was concluded that one of the most critical reasons for the cooling requirement is due to local hot spots [2]. For portable or unattended systems, passive solutions that operate without requiring any external energy source are attractive, and consist of liquid loops, pumps, plumping and parasitic energy. Today, the term passivity is used to describe the operation without sensors and controllers without electrical actuation power.

A second research stream is morphing structures, where structures are modified in their geometry to most adequately handle the operating conditions. A number of morphing aircraft concepts have been thoroughly explored and it has been proven that the key benefit of a morphing aircraft is the ability to satisfy conflicting requirements which are not possible with fixed geometry [3]. A similar conflict exists in the design of heat-sinks, a small, low aspect-ratio heat-sink would be suitable for an idle load, and a large, high aspect-ratio heat-sink would be suitable for a burst load. This review is then followed by an examination of the potential of the use of variable-geometry fins, which are biologically inspired and thermoactuated, for overcoming this conflict.

II. REVIEW SCOPE AND METHODOLOGY

The 26 sources analyzed were compared across 15 years of time (2002–2016) and were systematically reviewed with a protocol. All the sources were screened, coded and classified within the following thematic groups: constructal and bio-inspired design, PCM heat sinks and storage, conductivity enhancement, shape memory alloy (SMA) actuation and morphing and electronics thermal challenges. These groups were related to the constructal law: "In nature, flow systems tend to 'design' themselves to become more accessible to flow over time" [4]. As can be seen in Table I, the distribution of sources by concept mapping results in 5 concepts that have 1 to 7 sources, while the other concepts have no sources. Also, a thematic and temporal distribution as shown in Fig. 1 is obtained, with 8 sources out of 26 pointing towards PCM heat sinks, and 9 sources out of 26 being published between 2006 and 2009.

TABLE I. MAPPING OF REVIEWED LITERATURE TO DESIGN CONCEPTS

Thematic group	Core concept	Sources	Role in architecture
Constructal and bio-inspired design	Hierarchical, adaptive geometry	[4], [5], [6], [24], [25]	Fin geometry rules
PCM heat sinks and storage	Latent-heat buffering	[1], [8], [14], [17], [20], [21], [23], [26]	Transient energy sink

International Journal of Core Engineering & Management
Volume-7, Issue-04, 2022 ISSN No: 2348-9510

Thematic group	Core concept	Sources	Role in architecture
Conductivity enhancement	Foams, graphite, fillers	[7], [13], [15]	Conduction path to PCM
SMA actuation and morphing	Thermally driven geometry change	[3], [10], [11], [12], [16], [22]	Passive fin actuator
Electronics thermal challenges	Heat flux and hot spots	[2], [9], [18], [19]	Load definition

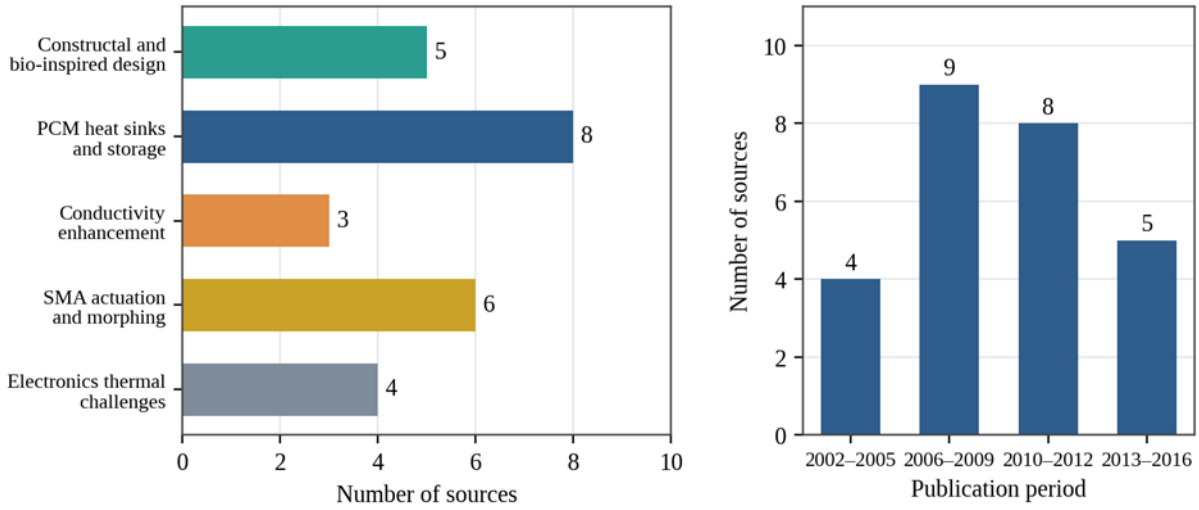


Fig. 1. Thematic and temporal distribution of the 26 reviewed sources.

III. BIO-INSPIRED AND CONSTRUCTAL FOUNDATIONS

Multi-scale "constructal" fin arrays are created as a first step to geometry inspired by nature for heat-sink applications. Arrays of pins with decreasing diameter and spacing were optimized on several length scales for a given volume and the resulting hierarchical structures were seen to give better heat transfer density than a uniform single-scale array [5]. It is found that the thermal performance of a given envelope is dependent on the geometry of the fins as well as the material and so the geometry of the fin can be seen as a design parameter, and may be changed as a function of load.

Adaptive geometry is a common phenomenon in biological structures for carrying out several different functions. A broad perspective of biomimetics identified these solutions and considered technology transfer not a copying of the form, but of the function [6]. Adaptive geometry is thus a frequent solution, which can be summarized in an engineering principle: Surface area and flow paths should be able to adjust to the current demand. Within the present context the rule translates to a compact fins when not in use and an expanded fins when a thermal burst is detected by the base temperature.

International Journal of Core Engineering & Management
Volume-7, Issue-04, 2022 ISSN No: 2348-9510

IV. TRANSIENT THERMAL MANAGEMENT WITH PHASE CHANGE MATERIALS

One of the common drawbacks of the organic PCMs is that they have low thermal conductivity ranging typically from 0.2 W/m•K, limiting the heat transfer across the melt front. The study of conductivity enhancement for thermal energy storage identified extended surface, high conductivity filler, and porous matrix as approaches and the penalty in energy stored due to additional solids as the key design trade-off [7]. The limitation is important for transient loads as the duration of the heating event is typically shorter than the time needed to conductively mobilize the entire PCM inventory.

The finned PCM heat sinks for portable hand-held electronics were studied experimentally and various fin numbers and dissipated power were investigated to determine the delay to reach a set-point temperature [8]. Fin performance is typically expressed as the fin efficiency of Eq. 1, in terms of the heat transfer coefficient h, fin perimeter P, fin conductivity k, and cross sectional area Ac, along with the fin length Lf. This is because it gets more inefficient as the fin gets longer, so there's an optimum length of a fixed fin for a fixed load, and this encourages a variable length fin.

$$\eta_f = \frac{\tanh(m_f L_f)}{m_f L_f} \qquad (1)$$

TABLE II. EXPERIMENTAL AND NUMERICAL PCM HEAT-SINK STUDIES IN THE REVIEWED SET

Source	Evaluation	Configuration	Principal finding
[1]	Experimental	PCM-filled finned heat sinks for electronics	Fins extend operating time before the set-point temperature
[8]	Experimental	Finned PCM heat sinks for hand-held devices	Fin number and power level govern the delay
[14]	Experimental and numerical	PCM-based heat sinks for portable electronics	Delay depends on power level and duty fraction
[17]	Experimental	Insert configurations with different PCM types	Insert layout and PCM type alter thermal response
[21]	Numerical	PCM heat sink with internal fins	Behavior organized by dimensionless parameters
[23]	Experimental	PCM cooling of mobile devices	Benefit is greatest for intermittent operation

Next generation electronic systems were discussed, focusing on thermal issues for the chip, package, and system, while non-uniform and time-varying power maps were identified as a significant cause of thermal design margin loss [9]. Thermal time constant in Eq. 2 describes the response of the heat-sink body to a sudden load.The thermal time constant in Eq. 2 indicates the

International Journal of Core Engineering & Management
Volume-7, Issue-04, 2022 ISSN No: 2348-9510

response of the heat-sink body to the sudden load, with Cth denoting the lumped thermal capacitance of the body in J/K, and G representing the heat transfer conductance from the body to the ambient in W/K. It has one time constant in the case of a fixed conductance and can be shortened in the load and extended in the idle case by an adaptive conductance.

$$\tau = \frac{C_{th}}{G} \qquad (2)$$

V. SHAPE MEMORY ALLOY ACTUATION

Shape memory alloys are alloys of metals that are able to return to their original shape when they are heated above a critical temperature, which is induced by a reversible solid-state phase transformation between two phases, the low-temperature martensite phase and the high-temperature austenite phase. The applications of SMAs in the aerospace were introduced, and the direct conversion of heat to motion (no motor, gears, or hydraulic lines) was demonstrated to be compact and lightweight in confined applications [10]. The same characteristics apply to heat sinks, where the volume is limited and there is a thermal signal at the actuation location.

A good example of such a precedent is the use of a Ni60Ti shape memory alloy for active jet engine chevrons, in which the trailing edge of the nozzle is thermally manipulated to alter its shape as the temperature of the surrounding air changes. The numerical analysis of the chevron was validated through experiments and it was demonstrated that prediction of the thermomechanical response is possible for a practical component [11]. As illustrated, passive morphing is possible without using electrical control, which is the key for this type of change.

A review of SMA research revealed NiTi-based alloys to be the most used family, and recoverable strains to be as high as 8 % and transformation temperatures to be shifted from about −100 °C to 100 °C by changing the composition [12]. The representative properties are gathered together in Table III. The volume fraction of austenite, ξ, is often assumed to be smooth as a sigmoidal curve of the form given by Eq. 3, where Tt is the austenite transformation temperature and w is a width parameter in kelvin. The heating and cooling follow different values of Tt and the resultant hysteresis is about 20-40 K as shown in Fig. 2.

$$\xi(T) = \frac{1}{1+exp\left(\frac{-(T-T_t)}{w}\right)} \qquad (3)$$

TABLE III. REPRESENTATIVE PROPERTIES OF NITI-BASED SHAPE MEMORY ALLOYS

Property	Representative value	Relevance to fin actuation
Recoverable strain	Up to about 8 %	Sets achievable fin deflection
Transformation temperature	About −100 °C to 100 °C	Tunable activation above idle temperature
Thermal hysteresis	20 K to 40 K	Defines the retraction temperature

International Journal of Core Engineering & Management
Volume-7, Issue-04, 2022 ISSN No: 2348-9510

Property	Representative value	Relevance to fin actuation
Density	About 6.45 g/cm³	Mass penalty of the actuator
Thermal conductivity	About 8.6 to 18 W/m·K	Speed of thermal coupling to the base

Note: Values are representative of NiTi-based alloys discussed in the reviewed SMA literature.

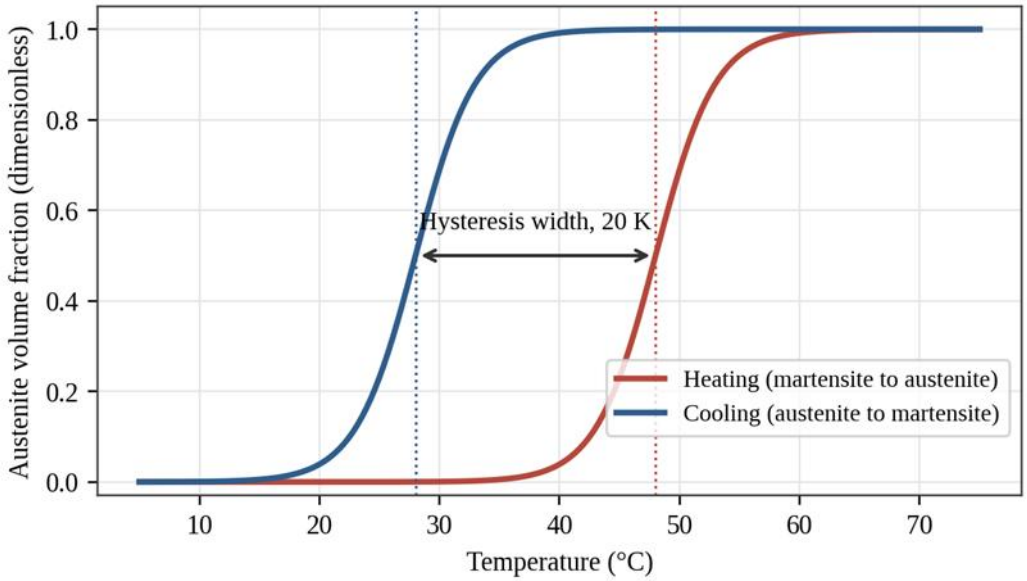


Fig. 2. Assumed sigmoidal transformation response of an SMA element with 20 K hysteresis.

VI. CONDUCTIVITY ENHANCEMENT OF PCM COMPOSITES

In a PCM, conductive scaffolds of ultrathin graphite foams were used and it was reported that the thermal conductivity of the composite could be significantly raised when compared with the neat material, and the latent heat per unit mass of the composite was not significantly lowered due to the very low solid loading [13]. The upper bound for the effective conductivity of a conductive matrix (solid volume fraction φ) is – for the parallel model – given by Eq. 4, where kPCM and ks are the conductivities of the PCM and the solid matrix. The enhancement approaches are compared in Table IV and the bound for three solid matrices are shown in Fig. 3.

$$k_{eff} = (1-\varphi)k_{PCM} + \varphi k_s \qquad (4)$$

International Journal of Core Engineering & Management
Volume-7, Issue-04, 2022 ISSN No: 2348-9510

TABLE IV. COMPARISON OF CONDUCTIVITY ENHANCEMENT APPROACHES

Approach	Mechanism	Conductivity estimate	Principal trade-off
Neat paraffin	None	About 0.2 W/m·K	Melt-front-limited conduction
Extended fins	Added surface area	Local to fin vicinity	Fin volume displaces PCM
Copper foam, 5 % solids	Percolating metal network	Up to 20.2 W/m·K	Mass and cost increase
Aluminum foam, 5 % solids	Percolating metal network	Up to 12.0 W/m·K	Lower gain than copper
Graphite foam, 5 % solids	Percolating carbon network	Up to 7.7 W/m·K	Fabrication complexity

Note: Foam values are parallel-path upper bounds computed from Eq. 4; realized values are lower.

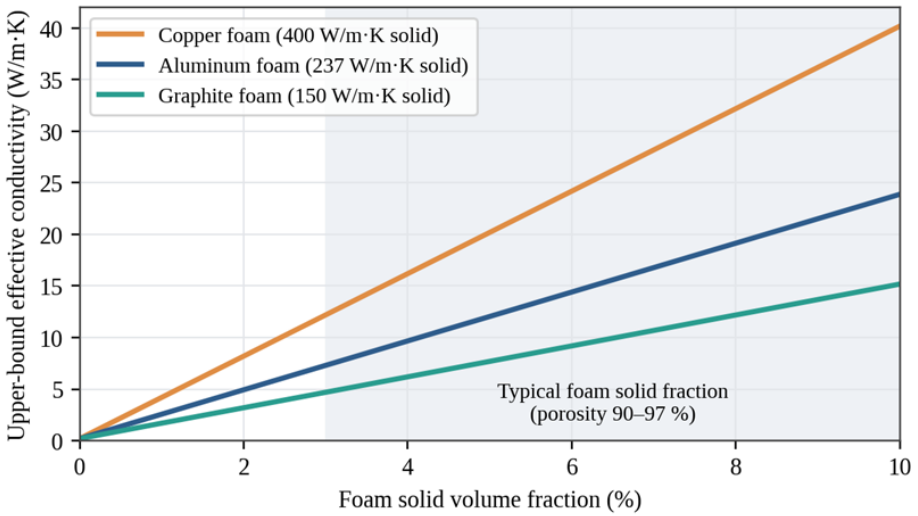


Fig. 3. Upper-bound effective conductivity of foam-PCM composites versus solid fraction.

A series of experiments were performed to test PCM-based heat sinks in portable electronics at various power levels and duty cycles, and the delay until a critical temperature was determined to be a function of both power dissipated and duty cycle [14]. The delay is proportional to the ratio of the latent capacity to the net heating power for a specific mass of a PCM. The remembrance of the observation is that the amount of energy stored in the PCM would have to equal the burst energy and for the 25 W pulse for 300 s, a reference load value of 7.5 kJ is used for further comparisons.

International Journal of Core Engineering & Management
Volume-7, Issue-04, 2022 ISSN No: 2348-9510

The effect of the foam porosity and pore size on PCM melting has been investigated experimentally and it was concluded that the melting behavior of PCM was different from that of pure PCM for both the parameters [15]. High-porosity foams (usually with porosities greater than 90 %) store the majority of the PCM while high-porosity promotes conduction, which occurs at the expense of storage. These geometry-dependent trade-offs would only become larger for a load that was using them, and a morphing structure would be able to modulate these trade-offs during use.

VII. PROPOSED PASSIVE MORPHING ARCHITECTURE

An edited book on modelling and engineering application [16] was compiled which includes constitutive modelling frameworks for SMAs, including the coupling with thermo-mechanical loads, the transformation kinetics and the design of actuators. The proposed idea to reduce the heat-sink is based on individual pivot/bends of each fin using SMA which is thermally coupled with the base. The conductance between the base and the PCM will then be represented by Eq. 5, where G0 is the conductance if the PCM is compacted and β is the deployment gain or ratio of conductance increase when the PCM is fully deployed. The 1.5 gain is when the conductance is 2.5.

$$G(T) = G_0[1 + \beta\xi(T)] \quad (5)$$

The performance of heat sinks with varying configurations and PCM types was determined experimentally and was found to give different heat-sink responses to a given heat power [17]. The proposed architecture can thus be considered as a reconfigurable device: compact fins at idle state will provide maximum PCM volume and minimum mass, whereas expanded fins post activation will penetrate the PCM and reduce conduction path lengths. The cycle can be repeated as the fins are compacted by reverse transformation when cooled.

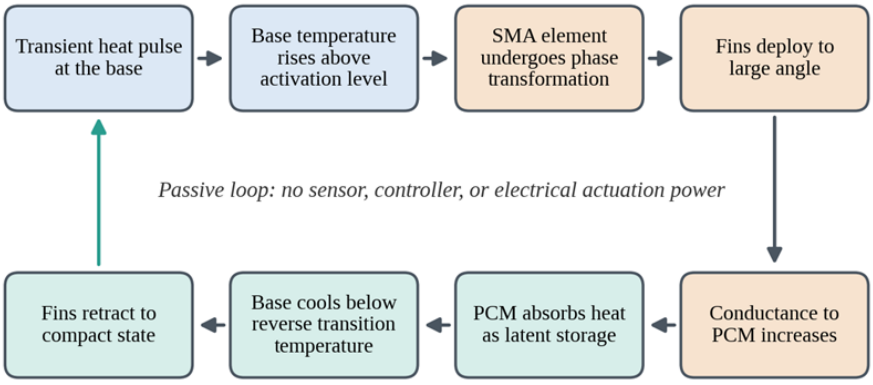


Fig. 4. Passive actuation loop of the proposed morphing heat-sink architecture.

Some emerging materials issues for electronics thermal management were examined, focusing on interfaces, high conductivity material development and reliability after repeated thermal cycles [18]. The most critical reliability issues for the proposed architecture are the thermal-cycle fatigue of the SMA element and the pivot interface as well as the contact resistance between the fins and the base. For material pairs, therefore, the activation temperature should be above the idle operating temperature, but below the device limit.

The energy dissipation and transport in nanoscale devices were analysed and the formation of localized hot spots at length scales much smaller than the heat sink were explained by the restrictions of the carrier and phonon transport [19]. The morphing heat sink is not intended to remove nanoscale hot spots, but rather the nanoscale transient hot spot that is caused by spreading at the package level.

VIII. COMPARATIVE ANALYSIS AND DISCUSSION

Thermal energy storage using PCMs was reviewed in terms of classes of materials, containment and application and it was found that organic Paraffins are chemically stable materials having moderate latent heat range of 150 kJ/kg to 250 kJ/kg [20]. The energy absorbed by a PCM mass m when the initial temperature of the PCM Ti is increased to the final temperature Tf is represented by Eq. 6, where cs and cl are the specific heat of the solid and liquid phases, respectively, of the PCM; Tm is the melting temperature of the PCM; L is the latent heat of fusion of the PCM; and γ is the fraction of the PCM in the liquid phase. When the temperature range is small (as in electronics), latent storage is the prevalent type of storage.

$$Q = m\left[c_s(T_m - T_i) + \gamma L + c_l(T_f - T_m)\right] \qquad (6)$$

A numerical study of PCM heat sinks with fined internal structures revealed that the heat behavior could be organized by dimensionless groups, and the Stefan number in Eq. 7 represented this ratio, which is the ratio of sensible capacity to latent capacity, where cl represents the capacity of the liquid and ΔT represents the difference of the temperature above melting [21]. The Stefan number for a paraffin with cl near 2.1 kJ/kg•K, L near 200 kJ/kg and ΔT near 15 K is about 0.16, which represents latent dominated storage and melt-front limited conduction.

$$Ste = \frac{c_l \Delta T}{L} \qquad (7)$$

A review of morphing aircraft using the smart materials and structures were conducted, while the actuation using shape memory material was compared to other smart material actuation options in terms of the achievable strain, applied force, bandwidth and complexity of the integration [22]. Such transfer of comparison led to the formulation of a lumped model of the proposed architecture based on the energy balance defined by Eq. 8, where Ch is the base-side

International Journal of Core Engineering & Management
Volume-7, Issue-04, 2022 ISSN No: 2348-9510

capacitance (30 J/K), P(t) is the heating power, Ga is the direct conductance to ambient (0.25 W/K), and Th, Ta, and Tp represent the base, ambient, and PCM temperature. A 40 g PCM charge (L = 200 kJ/kg, Tm = 40 °C, G0 = 1.0 W/K, β = 1.5) was subjected to 25 W for 300 s, with SMA transformation at 45 °C on heating and 30 °C on cooling. The results are indicative only and are tabulated in table V and plotted in figure 5.

$$C_h \frac{dT_h}{dt} = P(t) - G_a(T_h - T_a) - G(T_h)(T_h - T_p) \qquad (8)$$

TABLE V. LUMPED-MODEL COMPARISON OF THREE HEAT-SINK ARCHITECTURES

Architecture	Peak base temperature (°C)	Time to reach 55 °C (s)	Time above 55 °C (s)	PCM melted at 300 s (%)
Fixed fins without PCM	116.8	43	391	0
Fixed fins with PCM	57.0	117	186	41
Morphing fins with PCM	48.4	Not reached	0	49

Note: Illustrative model results for a 25 W, 300 s burst; the 55 °C limit is an assumed device constraint.

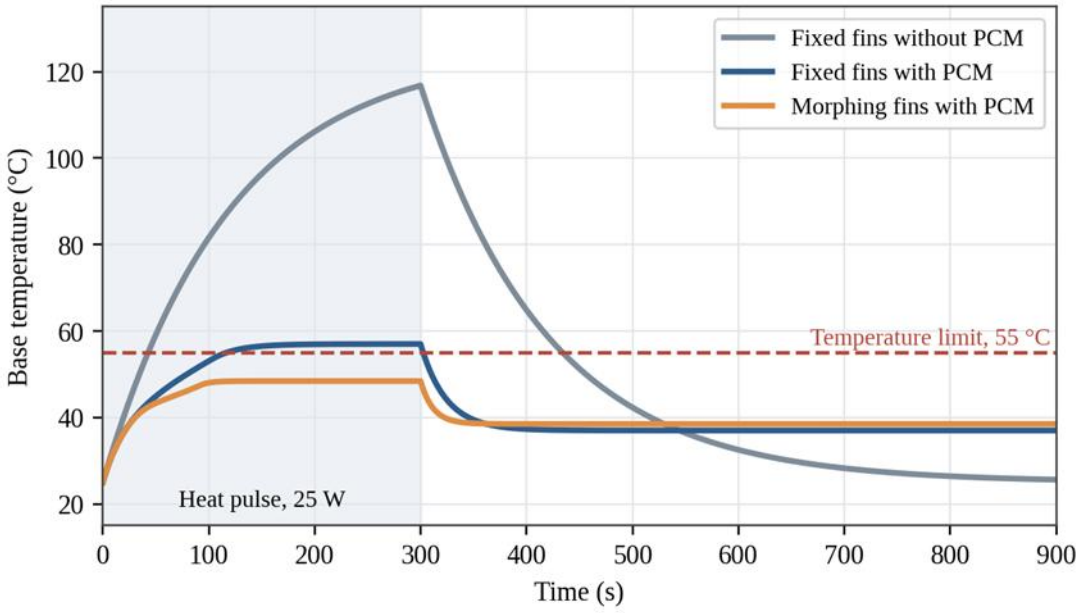


Fig. 5. Simulated base temperature during and after a 25 W, 300 s burst.

The cooling of mobile electronic devices by PCM was experimentally proven, and it was found that the PCM's most important advantage was the increase in the operating time between the cooling events without the need for additional fan power [23]. The lumped model consistently

International Journal of Core Engineering & Management
Volume-7, Issue-04, 2022 ISSN No: 2348-9510

shows that the peak base temperature decreases from 116.8 °C to 57.0 °C with respect to the unbuffered case with the fixed fins and 48.4 °C with the morphing configuration, which is 8.6 K less than the fixed fins (Fig. 6). The morphing base does not rise to 55 °C, while the fixed-fin base and the unbuffered base do for 186 s and 391 s, respectively. At the tail end of the burst, the melted fraction increases from 41 % to 49 % indicating better utilization of latent capacity.

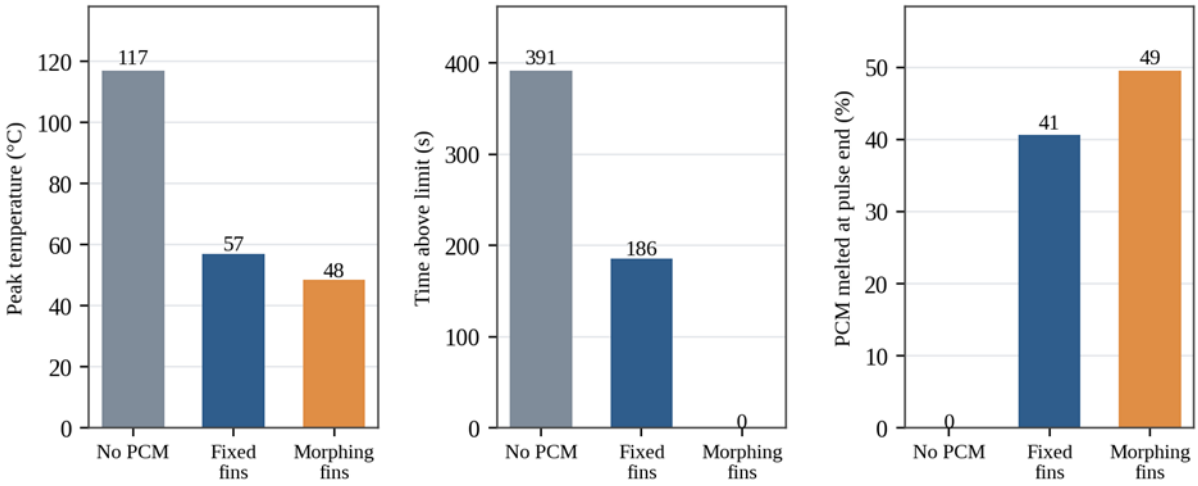


Fig. 6. Comparison of peak temperature, time above limit, and melted fraction.

Biomimetics was explored as a structured method, and the adoption of biological solutions to engineering problems was demonstrated to be most effective when the problem is first posed in terms of function, constraint, and scale in engineering rather than appearance [24]. When expressed in this way, the heat-sink problem becomes one of "is an object compact enough to still have a high conductance when loaded in time-varying fashion?": biological adaptive surfaces are analogues of this problem. The heat flow into the PCM can be increased by 150 % at the same temperature difference with a conductance rise from 1.0 W/K to 2.5 W/K at no actuation power.

Optimal tree-shaped networks for fluid flow in a disc-shaped body were derived, and a branching hierarchy was demonstrated to decrease the overall flow resistance compared with non-hierarchical networks [25]. The fine branches of a morphing array that follow the Murray-type diameter ratio in Eq. 9 get smaller at each bifurcation by a factor of 0.79, meaning that the sum of the cubes of the diameters remains constant at each bifurcation. Such a rule provides a quantitative guideline for the combination of hierarchical fin geometry and deployment.

$$\frac{D_{i+1}}{D_i} = 2^{-1/3} \qquad (9)$$

They reviewed TES using PMCM, heat transfer analyses and applications and practical barriers such as super cooling, containment and long-term cycling stability [26]. The barriers presented in the reviewed literature and mitigation directions proposed by the synthesis are summarized

in Table VI. The combined set of experimental results with SMA-actuated fins in PCM-filled enclosures during repeated bursts is lacking overall.

TABLE VI. PRINCIPAL BARRIERS AND MITIGATION DIRECTIONS

Barrier	Source	Evidence in review	Mitigation direction
Low PCM conductivity	[7]	About 0.2 W/m·K for organic PCMs	Foams, fins, graphite scaffolds
Supercooling and cycling stability	[26]	Documented for PCM storage	Material screening, nucleating agents
SMA hysteresis	[12]	20 K to 40 K typical	Set cooling transformation above idle level
Fatigue and interface resistance	[18]	Concern under thermal cycling	Limit strain, qualify interfaces
Lack of validation	[11]	Validated for chevrons, not heat sinks	Prototype testing under repeated bursts

IX. CONCLUSION

This review combined 26 sources to form a passive morphing heat-sink structure that increases the conductance to a phase change material during transients. The comparative lumped analysis revealed a maximum base temperature of 48.4 °C in case of morphing fins as compared to 57.0 °C and 116.8 °C for the fixed fins in the case of storage and without storage respectively, along with higher melted fraction of 49 % as compared to 41 % for the case of fixed fins. Conduction bounds of 7.7 W/m•K to 20.2 W/m•K for foam composites demonstrate that passive means can be used to alleviate conduction limits. Subsequent work priorities include experimental prototypes, fatigue characterization and optimization of fin hierarchy.

REFERENCES

1. R. Baby and C. Balaji, “Experimental investigations on phase change material based finned heat sinks for electronic equipment cooling,” International Journal of Heat and Mass Transfer, vol. 55, no. 5–6, pp. 1642–1649, 2012, doi: 10.1016/j.ijheatmasstransfer.2011.10.047.
2. A. Bar-Cohen, M. Arik, and M. Ohadi, “Direct liquid cooling of high flux micro and nano electronic components,” Proceedings of the IEEE, vol. 94, no. 8, pp. 1549–1570, 2006, doi: 10.1109/JPROC.2006.879791.
3. S. Barbarino, O. Bilgen, R. M. Ajaj, M. I. Friswell, and D. J. Inman, “A review of morphing aircraft,” Journal of Intelligent Material Systems and Structures, vol. 22, no. 9, pp. 823–877, 2011, doi: 10.1177/1045389X11414084.

4. A. Bejan and S. Lorente, "The constructal law and the evolution of design in nature," Physics of Life Reviews, vol. 8, no. 3, pp. 209–240, 2011, doi: 10.1016/j.plrev.2011.05.010.
5. T. Bello-Ochende, J. P. Meyer, and A. Bejan, "Constructal multi-scale pin-fins," International Journal of Heat and Mass Transfer, vol. 53, no. 13–14, pp. 2773–2779, 2010, doi: 10.1016/j.ijheatmasstransfer.2010.02.032.
6. B. Bhushan, "Biomimetics: Lessons from nature—an overview," Philosophical Transactions of the Royal Society A, vol. 367, no. 1893, pp. 1445–1486, 2009, doi: 10.1098/rsta.2009.0011.
7. L. Fan and J. M. Khodadadi, "Thermal conductivity enhancement of phase change materials for thermal energy storage: A review," Renewable and Sustainable Energy Reviews, vol. 15, no. 1, pp. 24–46, 2011, doi: 10.1016/j.rser.2010.08.007.
8. S. C. Fok, W. Shen, and F. L. Tan, "Cooling of portable hand-held electronic devices using phase change materials in finned heat sinks," International Journal of Thermal Sciences, vol. 49, no. 1, pp. 109–117, 2010, doi: 10.1016/j.ijthermalsci.2009.07.005.
9. S. V. Garimella, A. S. Fleischer, J. Y. Murthy, A. Keshavarzi, R. Prasher, C. Patel, S. H. Bhavnani, R. Venkatasubramanian, R. Mahajan, Y. Joshi, B. Sammakia, B. A. Myers, L. Chorosinski, M. Baelmans, P. Sathyamurthy, and P. E. Raad, "Thermal challenges in next-generation electronic systems," IEEE Transactions on Components and Packaging Technologies, vol. 31, no. 4, pp. 801–815, 2008, doi: 10.1109/TCAPT.2008.2001197.
10. D. J. Hartl and D. C. Lagoudas, "Aerospace applications of shape memory alloys," Proceedings of the Institution of Mechanical Engineers, Part G: Journal of Aerospace Engineering, vol. 221, no. 4, pp. 535–552, 2007, doi: 10.1243/09544100JAERO211.
11. D. J. Hartl, J. T. Mooney, D. C. Lagoudas, F. T. Calkins, and J. H. Mabe, "Use of a Ni60Ti shape memory alloy for active jet engine chevron application: II. Experimentally validated numerical analysis," Smart Materials and Structures, vol. 19, no. 1, Art. no. 015021, 2010, doi: 10.1088/0964-1726/19/1/015021.
12. J. M. Jani, M. Leary, A. Subic, and M. A. Gibson, "A review of shape memory alloy research, applications and opportunities," Materials & Design, vol. 56, pp. 1078–1113, 2014, doi: 10.1016/j.matdes.2013.11.084.
13. H. Ji, D. P. Sellan, M. T. Pettes, X. Kong, J. Ji, L. Shi, and R. S. Ruoff, "Enhanced thermal conductivity of phase change materials with ultrathin-graphite foams for thermal energy storage," Energy & Environmental Science, vol. 7, no. 3, pp. 1185–1192, 2014, doi: 10.1039/C3EE42573H.
14. R. Kandasamy, X.-Q. Wang, and A. S. Mujumdar, "Application of phase change materials in thermal management of electronics," Applied Thermal Engineering, vol. 27, no. 17–18, pp. 2822–2832, 2007, doi: 10.1016/j.applthermaleng.2006.12.013.
15. K. Lafdi, O. Mesalhy, and S. Shaikh, "Experimental study on the influence of foam porosity and pore size on the melting of phase change materials," Journal of Applied Physics, vol. 102, no. 8, Art. no. 083549, 2007, doi: 10.1063/1.2802184.
16. D. C. Lagoudas, Ed., Shape Memory Alloys: Modeling and Engineering Applications. Springer, 2008, doi: 10.1007/978-0-387-47685-8.

17. S. Mahmoud, A. Tang, C. Toh, R. Al-Dadah, and S. L. Soo, "Experimental investigation of inserts configurations and PCM type on the thermal performance of PCM based heat sinks," Applied Energy, vol. 112, pp. 1349–1356, 2013, doi: 10.1016/j.apenergy.2013.04.059.
18. A. L. Moore and L. Shi, "Emerging challenges and materials for thermal management of electronics," Materials Today, vol. 17, no. 4, pp. 163–174, 2014, doi: 10.1016/j.mattod.2014.04.003.
19. E. Pop, "Energy dissipation and transport in nanoscale devices," Nano Research, vol. 3, no. 3, pp. 147–169, 2010, doi: 10.1007/s12274-010-1019-z.
20. A. Sharma, V. V. Tyagi, C. R. Chen, and D. Buddhi, "Review on thermal energy storage with phase change materials and applications," Renewable and Sustainable Energy Reviews, vol. 13, no. 2, pp. 318–345, 2009, doi: 10.1016/j.rser.2007.10.005.
21. V. Shatikian, G. Ziskind, and R. Letan, "Numerical investigation of a PCM-based heat sink with internal fins," International Journal of Heat and Mass Transfer, vol. 48, no. 17, pp. 3689–3706, 2005, doi: 10.1016/j.ijheatmasstransfer.2004.10.042.
22. J. Sun, Q. Guan, Y. Liu, and J. Leng, "Morphing aircraft based on smart materials and structures: A state-of-the-art review," Journal of Intelligent Material Systems and Structures, vol. 27, no. 17, pp. 2289–2312, 2016, doi: 10.1177/1045389X16629569.
F. L. Tan and C. P. Tso, "Cooling of mobile electronic devices using phase change materials," Applied Thermal Engineering, vol. 24, no. 2–3, pp. 159–169, 2004, doi: 10.1016/j.applthermaleng.2003.09.005.
23. J. F. V. Vincent, O. A. Bogatyreva, N. R. Bogatyrev, A. Bowyer, and A.-K. Pahl, "Biomimetics: Its practice and theory," Journal of the Royal Society Interface, vol. 3, no. 9, pp. 471–482, 2006, doi: 10.1098/rsif.2006.0127.
24. W. Wechsatol, S. Lorente, and A. Bejan, "Optimal tree-shaped networks for fluid flow in a disc-shaped body," International Journal of Heat and Mass Transfer, vol. 45, no. 25, pp. 4911–4924, 2002, doi: 10.1016/S0017-9310(02)00208-4.
25. B. Zalba, J. M. Marín, L. F. Cabeza, and H. Mehling, "Review on thermal energy storage with phase change: Materials, heat transfer analysis and applications," Applied Thermal Engineering, vol. 23, no. 3, pp. 251–283, 2003, doi: 10.1016/S1359-4311(02)00192-8.